Embedded Driver-Assistance System Using Multiple Sensors for Safe Overtaking Maneuver

Hsin-Han Chiang, *Member, IEEE,* Yen-Lin Chen, *Senior Member, IEEE,* Bing-Fei Wu, *Fellow, IEEE,* and Tsu-Tian Lee, *Fellow, IEEE*

***Abstract*—Advanced driver-assistance systems have recently become one of the most active topics related to intelligent vehicles. Such assistance facilitates vehicular operation by allowing drivers increased control and an enhanced driving experience, and it even comes in the form of automated assistance for autonomous vehicle operation. This paper presents a driver-assistance system that uses a low-cost embedded digital signal processor, with the overall system installed in a commercial vehicle. Based on driving information supplied by multiple sensors, such as a real-time vision system, a vehicle-to-vehicle communication system, and in-vehicle sensors, the proposed system can facilitate decision making and the performing of driving tasks while executing overtaking maneuvers. This paper developed a data fusion stage based on a collision warning algorithm in which the overtaken vehicle and other vehicles in the neighboring lane are accounted for to avoid collisions. The system employs fuzzy control in the steering and speed automation to emulate the driving tasks performed by humans. The applicability of the proposed system was examined in a real-road environment, and a set of experimental results demonstrate the feasibility of using the involved coordination strategies while conducting various driving maneuvers.**

***Index Terms*—Collision avoidance, digital signal processor (DSP), driver-assistance systems, intelligent vehicles, overtaking maneuver.**

I. Introduction

INTELLIGENT vehicles (IVs) integrate various technologies, including sensors, communication, and computing techniques, with electronic devices to improve the diverse fields of the transportation domain, thereby augmenting driving safety, convenience, and comfort. Investigating advanced vehicle control and safety systems has become the key development within IVs research fields and the automotive industry [1]. The ultimate purpose of such investigation is to implement various types of driving-assistance systems, providing an opportunity to relieve the driver from driving fatigue and the monotonous routines of driving tasks. Among these tasks, lane-keeping and lane-change maneuvers are used as primitives for performing complex operations such as avoiding obstacles or overtaking vehicles ahead [2]–[18]. Previous studies have widely admitted that the overtaking maneuver causes numerous fatal crashes because of the unsafe diversion space from the original lane, poor visibility when passing a vehicle, or erroneous judgment in returning to the lane [12]–[15], [18]–[20].

A safe overtaking maneuver entails passing a slower-moving vehicle ahead on a two-way lane. However, the most critical factors of overtaking maneuvers should comprise the following: a safe distance to the vehicle to be overtaken when initiating the overtaking operation, an adequate period for each lane-change maneuver, accounting for varied road widths, a smooth and comfortable lane-change trajectory, and safely returning to the original lane or maintaining a safe headway from a vehicle ahead when the overtaking maneuver cannot be executed. Consequently, such systems require the capability to assess the current traffic situation and to manage the speed and steering in a coordinated manner, thereby minimizing collision risk with neighboring vehicles.

Because of the rapid developments of the system-on-chip technique, embedded systems that can effectively bridge the gap between control theory and real-time implementation have popularized research in the field of intelligent control systems [22]–[24]. A mathematical framework is proposed in [25] for analyzing embedded system functional flexibility quantitatively. To accomplish an efficient portable solution for driving assistance, this paper presents an embedded driver-assistance system, which possesses the functionalities of lane keeping, lane changing, and overtaking maneuvers. We implemented the control system using a digital signal processor (DSP) for real-time computation in using various sensors and controlling the steering wheel, throttle, and brake actuators. This paper discusses theoretical aspects as well as practical demonstrations and real-road tests. Moreover, the challenges of performing complicated overtaking maneuvers involve coordinating separate driving controls, as well as the real-time integration of heterogeneous and complex systems, such as the vision system, vehicle-to-vehicle (V-V) communication system, embedded controller, and in-vehicle sensors

Manuscript received January 14, 2012; revised May 6, 2012, July 3, 2012 and July 16, 2012; accepted July 30, 2012. Date of publication November 16, 2012; date of current version August 21, 2014. This work was supported by the National Science Council of Taiwan under Grants NSC-100-2221-E-027-033, NSC-100-2221-E-030-004, and NSC-101-2219-E-027-006.

H.-H. Chiang is with the Department of Electrical Engineering, Fu Jen Catholic University, New Taipei City 24205, Taiwan (e-mail: hsinhan@ee.fju.edu.tw).

Y.-L. Chen is with the Department of Computer Science and Information Engineering, National Taipei University of Technology, Taipei 10608, Taiwan (e-mail: ylchen@csie.ntut.edu.tw).

B.-F. Wu is with the Institute of Electrical and Control Engineering, National Chiao Tung University, Hsinchu 30050, Taiwan (e-mail: bwu@cssp.cn.nctu.edu.tw).

T.-T. Lee is with the Department of Electrical Engineering, Chung Yuan Christian University, Taoyuan 32023, Taiwan (e-mail: ttlee@cycu.edu.tw).

Color versions of one or more of the figures in this paper are available online at http://ieeexplore.ieee.org.

Digital Object Identifier 10.1109/JSYST.2012.2212636

and actuators. The remainder of this paper is as follows. A review of literature in the area of driver-assistance systems in IVs is presented in Section II, particularly emphasizing active driver support. Section III introduces the system configuration and Section IV describes the driver-assistance system design responsible for the overtaking maneuver. Section V presents the implementation of our system into an embedded platform. The experimental results are provided and some system bottleneck issues are discussed in Section VI. Finally, Section VII presents discussion and conclusions.

II. Related Works in IVs

In recent decades, automated vehicles have drawn considerable attention, particularly because of lateral control and automatic steering. The Navigation Laboratory (NavLab) at Carnegie Mellon University has developed automated steering controllers for their NavLab vehicle series, based on an artificial vision system and controlled by the rapidly adapting lateral position handler [2], [3]. Prof. Alberto Broggi and his team at Parma University in Italy developed the ARGO vehicle using stereo vision as an image-detecting device to obtain information from the road ahead, as well as a personal-computer-based control system to manage the steering wheel automatically when engaged in lane-keeping and lane-change tasks [4], [5]. In the California Partners for Advanced Transit and Highways Program, Hessburg and Tomizuka proposed a lateral vehicle guidance system based on a fuzzy control approach and implemented it in a Toyota Celica experimental test vehicle [6]. In this program, lane-change maneuvers are executed using diverse approaches. Swaroop *et al.* at Texas A&M University presented an automatic lane-change maneuver to respond to contingencies such as obstacle avoidance [7]. Furthermore, previous studies have presented the lane-change maneuver as the starting point for improving lane-change control system efficiency within platoon operations [8]–[11]. In the AUTOPIA Program, two Citroen Berlingo vans equipped with a fuzzy logic-based control system to mimic human driving behavior were proposed to provide path-tracking and lane-change capabilities in urban-like environments [15]. An automated steering system using mainly the vision system was implemented at National Chiao Tung University [16]. The DARPA Urban Challenge, a completely autonomous vehicle race, was held in 2007 in mock city environments. The vehicles contended against one another, performing complex maneuvers such as the following: passing or overtaking vehicles, leaving or merging into moving traffic, and navigating through parking lots [17]. In the recent European Project HAVEit, cooperation between the driver and a copilot system has drawn more attention toward automation modes varying from fully human to highly automated [21]. Thus far, numerous automated driving systems have been developed; however, real-time obstacles involving complete longitudinal and lateral vehicle control have yet to be overcome. Instead of representing the vehicle system as a set of complex mathematical equations, many studies in this field have advocated designing fuzzy controllers, because the empirical rules can be represented by the input and output relationships of the system with the availability of human expert knowledge [6], [13]–[16], [20], [22], [27], [28]. Although the effectiveness of fuzzy-based vehicle control can be demonstrated, the stability difficulties of control systems remain unresolved.

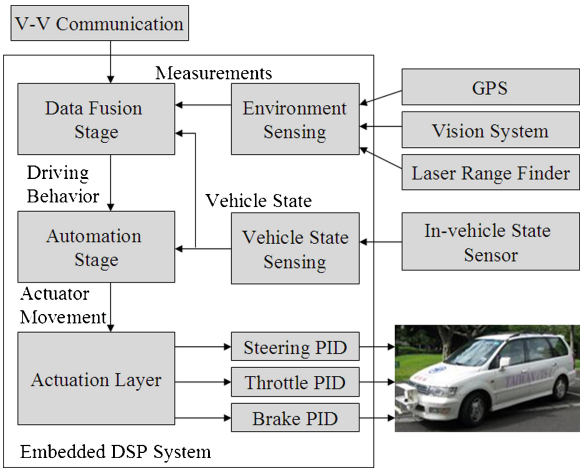

Fig. 1. System architecture of the embedded copilot system with the testbed vehicle.

The overtaking maneuver comprises a sequence of lane-change and lane-keeping operations, i.e., it requires overtaking the vehicle by steering from the original lane into the adjacent lane, circulating in the adjacent lane, and returning to the original lane in front of the overtaken vehicle. Consequently, the overtaking maneuver is more complicated than other driving maneuvers because of the switch between several lane-keeping and lane-change processes, during which such a system must coordinate the vehicle's steering and speed to eliminate the potential of colliding with other vehicles. Hence, a mathematical model presenting a smooth and comfortable lane-change trajectory was proposed [19]. Another approach uses guidance-based online trajectory planning for simulation purposes [20]. However, few studies have investigated the more complicated overtaking processes that consider human-driven vehicles in the adjacent lane. Therefore, this paper proposes a safe overtaking maneuver in which human-driven vehicles are modeled using primitive driving dynamics such as braking and acceleration. Based on this maneuver, the vehicle equipped with our system determines in real time the current driving mode and performs the least restrictive safe control actions. Our approach leads to less conservative safety in the overtaking operation than those that treat human-driven vehicles as enemies to be counteracted in the worst-case scenario.

III. System Description

Fig. 1 shows the system architecture of the proposed system, exhibiting layered and feedback structures. The system design is based on a hierarchical architecture, which accords with the perspective of the behavioral psychology of drivers [26]. The higher level is designed for evaluating the necessity and feasibility of overtaking vehicles, providing a reference trajectory in executing lane-keeping and lane-change processes.

The reference speed is calculated to maintain the vehicle at a preset speed or at a safe distance from the lead vehicle when overtaking is not permitted. The lower level consists of the steering wheel controller and speed controller, which are designed based on fuzzy logic control (FLC) to provide an alternative approach for negotiating the uncertainty and complexity of the vehicle system, as well as imitating a human driver while steering and managing speed.

The testbed vehicle is supported by add-on hardware devices and processing software to fulfill the steering wheel control and speed control (throttle and braking actuation). The sensors, actuators, and core processor are described as follows.

A. Sensor Installation

The vehicle internal states, namely, velocity, acceleration, and yaw motion rate, are sensed by the speedometer and an inertia measurement unit (IMU). The relative distance and velocity information between the subject vehicle and the vehicle in front is measured by a laser range finder mounted on the subject vehicle's front frame. The vision system detects the lane markings ahead of the subject vehicle, and provides look-ahead road information, such as the lateral offset relative to the centerline of the road, yaw angle with respect to the road tangent, and road width [29], [30]. The V-V communication system with a differential global position system and wireless RS-232 transceiver (RF3105) is used to gather the relative distance and velocity from the vehicle in the adjacent lane involved in the overtaking operation.

B. Actuator Installation

For steering wheel actuation, an ac servomotor is installed in the steering column and its absolute rotary angle is measured by a steering angle encoder mounted on the steering rack. Such a system can provide power steering when the vehicle is under system-controlled mode. As for speed control, a throttle valve is driven by a mounted dc servomotor avoiding any change to the vehicle's internal components. A throttle position sensor is composed of an analog-to-digital (A/D) converter, encoding an analog voltage into a normalized digital signal. The brake pedal is automated using a dc servomotor connected to a brailed steel cable via an electromagnet. The position of the brake pedal is measured regarding the voltage variation from a linear position transducer.

C. System Core

Driver-compatible intelligence and behavior is incorporated into the embedded system, which performs the function of a system core for executing lane-keeping, lane-change, and overtaking maneuvers. A DSP TMS320F2812, a 32-b fixed-point DSP controller with on-board Flash memory provided by Texas Instruments (TI), is used on the eZdsp board for real-time implementation of the embedded system. The advantages of high-speed (150 millions of instructions per second) processing and multiple pulse-width modulation are appropriate for multiple-motor control, as well as for complex algorithms, such as FLC, and can be adequately applied to the servo system to improve control performance.

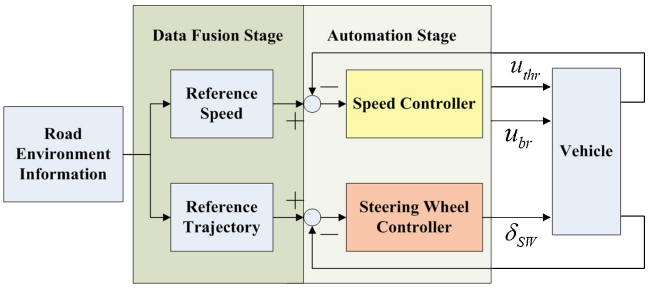

Fig. 2. Structure of controller/vehicle system.

The embedded system possesses two types of submodules, sensing and controller submodules, as shown in Fig. 1. Environmental data for vehicle operation are obtained from the vision system, V-V communication, and laser range finder; in-vehicle states obtained from the vehicle speed sensor and IMU are gathered by sensing modules via several RS-232 serial interfaces. The module of the data fusion stage determines the driving behavior, whereas that of the automation stage drives the steering, throttle, and brake motors over the A/D links. By receiving the throttle-, brake-position, and steering-commands from the vehicle body control, proportional-integral-differential (PID) controllers are applied to manage two dc motors (to adjust the throttle and brake degree) and one ac motor (to move the steering wheel toward its target position).

IV. System Design

The proposed system is designed as a hierarchical architecture, composed of two levels (Fig. 2), and can support automatic driving with various types of driving maneuvers. Without challenging the physical limits of the vehicle, a decoupled longitudinal and lateral control can be used to guide the vehicle through different driving maneuvers [8], [15], [31]. Moreover, based on observing the driving behavior of humans, the driver adopts a switching mechanism based on simple control laws instead of complex nonlinear control laws [32]. This switching mechanism and the auxiliary control laws can be regarded as the model of the driver's behavior involved in situational assessment (the data fusion stage) and physical skills (the automation stage), respectively.

The data fusion stage manages the sequence of operations to be executed, i.e., it determines the reference trajectory and reference speed involved in lane keeping, lane change, and overtaking. In lane keeping, the reference trajectory is well defined to maintain the lateral error at zero; at that instant, the reference speed depends strongly on the longitudinal motion of the vehicle. While assuming that the vehicle is steered under normal conditions, the driver in both the lane-change task and overtaking task often maintains a velocity with less fluctuation. In addition, the reference trajectory in the overtaking maneuver does not depend on the velocity of the overtaken vehicle but only on the point of initiating the diversion [19], [21]. Thus, longitudinal (speed) and lateral (trajectory) guidance can be separated.

The automation stage was designed using the FLC to incorporate human procedural knowledge into the control

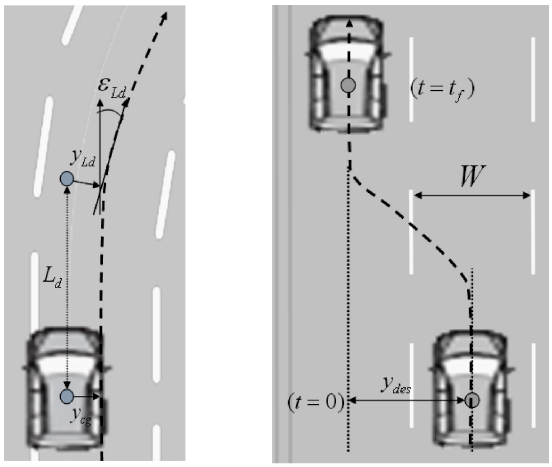

Fig. 3. Road model and reference trajectory for (a) lane-keeping and (b) lane-change maneuver.

algorithms of the speed and steering wheel controller layer. Because the longitudinal and lateral vehicle dynamics can be decoupled in a small velocity variation, this preserved linearity of dynamics can allow a separation design for longitudinal and lateral motion control [6], [8], [16], [19], [21], [31]. Accordingly, the speed controller maintains the reference speed as precisely as possible, whereas the steering wheel controller maintains the lateral error at zero, i.e., the steering wheel controller causes the subject vehicle to travel along the reference trajectory guided in the data fusion stage. Notably, both stages are designed to be adaptive to vehicle states such as current speed, real-time lateral error, and relative distance with respect to vehicles involved in different driving modes; this accounts for the fact that human drivers perform driving tasks adaptively, regarding these vehicle states.

A. Data Fusion Stage

1) *Reference Trajectory Generation:* The lane-keeping task entails maintaining the vehicle in the center of the lane. In this task, the control objective is to maintain the lateral error at zero; thus, the reference trajectory is the centerline of the road, which can be recognized by the vision system. Given a previewed range of the vehicle trajectory at a distance ahead of the vehicle, a parabolic lane model, which incorporates position, angle, and curvature, is commonly used in the construction of roads, as shown in Fig. 3(a). This lane model outputs the previewed data regarding the lateral offset and orientation with respect to the centerline of the detected lane [16], [29]

$$y_{Ld}(L_d) = kL_d^2 + m_0 L_d + b_0$$
$$\varepsilon_{Ld}(L_d) = 2kL_d + m_0 \tag{1}$$

where L_d represents the look-ahead distance of the vehicle, and k, m_0, and b_0 are the coefficients of the parabolic model.

A lane-change maneuver can be viewed according to the vehicle traveling a specified distance along the lateral axis with respect to its body orientation within a finite period, as shown in Fig. 3(b). After the vehicle has aligned itself with the adjacent lane at the end of the lane-change maneuver, the lane-keeping maneuver is resumed. By considering the vehicle as a mass point, the simplified model for the lateral trajectory of a vehicle navigating to the adjacent lane, as shown in Fig. 3(b), can be presented as

$$\dot{y}_{cg} = v_{cg},\ \dot{v}_{cg} = a_{cg},\ \dot{a}_{cg} = J_{cg} \tag{2}$$

where y_{cg} denotes the lateral displacement of the vehicle's CG with respect to the original lane center, and J_{cg} denotes the lateral jerk, which is the time derivative of the lateral acceleration a_{cg}.

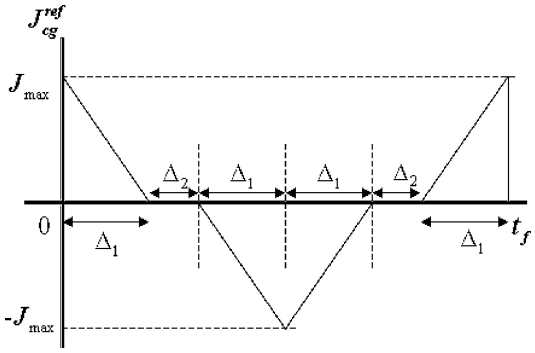

Fig. 4. Desired lateral jerk reference signal for the reference trajectory specification in the lane-change maneuver.

Initially assuming that $y_{cg}(t) = v_{cg}(t) = a_{cg}(t) = 0$ at $t = 0$ represents ideal lane keeping on the original road and, at the end of the lane-change maneuver ($t = t_f$), the condition $y_{cg}(t_f) = y_{\text{des}}$ should be achieved using $v_{cg}(t_f) = a_{cg}(t_f) = 0$, which is also required for proceeding with the lane-keeping maneuver. The steering angle of the vehicle should change sign twice during the interval [0, t_f] of the lane-change maneuver so that both the lateral jerk and lateral acceleration of the vehicle must be bounded. By adopting an analysis similar to that of [11], the desired trajectory for the lateral displacement of the vehicle can be generated from a reference signal of lateral jerk, as illustrated in Fig. 4. The final lateral travel y_{des} from the original lane to the adjacent lane is given by

$$y_{\text{des}} = \int\int\int J_{cg}^{\text{ref}}(\tau)d\tau d\psi dt$$
$$= \frac{J_{\max}}{12}\Delta_1(16\Delta_1^2 + 20\Delta_1\Delta_2 + 6\Delta_2^2). \tag{3}$$

In the lane-change maneuver, the vehicle moves from the centerline in the original lane to the alternative centerline located in the contiguous lane. Thus, the desired final value for y_{des} should be equal to the lane width W, which can be obtained using the vision system. Given the desired lateral displacement $y_{\text{des}} = W$, the absolute bounds on the lateral acceleration $A_{\max}$, and the jerk $J_{\max}$, (3) can be solved for Δ_1 and Δ_2. During the transition from one lane to another, the vision system fails to provide preview information because of the discontinuities of valid lane markings (as discussed in Section VI). This causes an open-loop transition period that must be minimized for the vehicle to return to the lane-keeping mode as soon as possible. To minimize the total period of $T = 4\Delta_1 + 2\Delta_2$, Δ_2 can be set at zero in (3)

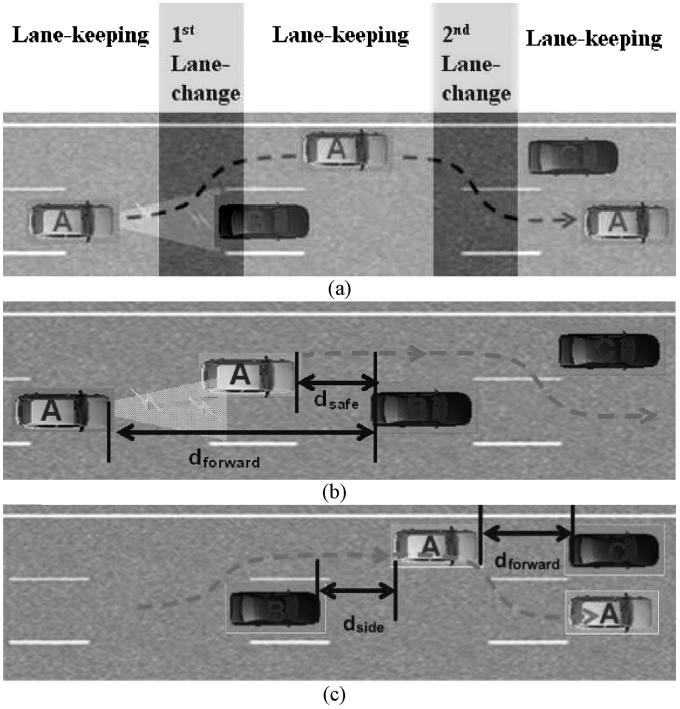

Fig. 5. Overtaking maneuver phases. (a) Overtaking maneuver using the lane-keeping and lane-change operation. (b) First phase of lane changing to the adjacent left lane. (c) Second phase of lane changing returning to the right lane.

to obtain $\Delta_1 = \sqrt[3]{3W/4J_{\max}}$. Furthermore, during the lane-change maneuver, lateral acceleration should also be bounded for ride quality consideration, i.e., $J_{\max} \cdot \Delta_1/2 = A_{\max}$. The value of Δ_1 can then be determined from

$$\Delta_1 = \min\left\{\frac{2A_{\max}}{J_{\max}}, \sqrt[3]{\left|\frac{3W}{4J_{\max}}\right|}\right\} \tag{4}$$

and Δ_2 is the minimum real positive root of Δ_2 found from solving (3), or equal to zero if there are no positive real roots. Given the ideal lateral jerk, acceleration, and lateral displacement, as represented in (2), the vehicle can perform a lane-change maneuver while preserving the ride comfort constraint.

Remark: $A_{\max}$ and $J_{\max}$ can be initially set in the system, and their values are generally within 0.2 g and 0.1 g/s, respectively, where g is the gravitational acceleration. The value of y_{des} is then used to determine the required durations Δ_1 and Δ_2. Note that it may be divergent, depending on the width of the road. By detecting the projective width between the left and the right lane markings on the image, the road width W can be rapidly estimated using our vision system [29]. Thus, the developed lane-change maneuver can be adapted to the road according to varied width.

The overtaking maneuver, as shown in Fig. 5(a), is composed of lane-keeping and lane-change tasks. Initially, the subject vehicle executes lane keeping and switches to the first lane change until closing on the forward vehicle. When the first lane change is complete, the subject vehicle performs the lane-keeping task in the adjacent lane. After passing the overtaken vehicle, the system performs the second lane change to the initial lane of the road and switches to lane keeping. If the lane is not long enough to execute the second lane change (i.e., if a slower lead vehicle appears or the overtaken vehicle accelerates, then the second lane change is not activated and the subject vehicle must decelerate to follow the vehicle in front at a safe distance). Consequently, the relative distance between the subject vehicle and the overtaken vehicle must be thoroughly considered when executing the overtaking maneuver to prevent collisions. Generally, emergency braking is a means for yielding a larger space between the vehicles involved so that every vehicle can stop without colliding at any time before, during, or after the overtaking maneuver. Because emergency braking can be activated at any time in a situation where the vehicle must decelerate for an emergency stop to avoid striking the vehicle ahead, the concept of rear-end collision avoidance should be applied to the vehicle's braking capability. Using Mazda and Honda's algorithm [33], a nondimensional warning value is defined as

$$I_w = \frac{d_r - d_{br}}{d_w - d_{br}} \tag{5}$$

where d_r is the measured intervehicular spacing, and d_w and d_{br} are the conservative warning distance and nonconservative braking distance, respectively, defined as

$$d_w = f(\mu) \cdot g(\phi_d) \cdot d_{w0} \tag{6}$$

$$d_{br} = f(\mu) \cdot g(\phi_d) \cdot d_{br0} \tag{7}$$

$$d_{w0} = v\tau + \left(\frac{v^2}{2a} - \frac{(v - v_{rel})^2}{2a^-_{\max}}\right) + d_0 \tag{8}$$

$$d_{br0} = v_{rel}\tau + \frac{1}{2}a^-_{\max}\tau^2 \tag{9}$$

where $f(\cdot)$ and $g(\cdot)$ represent the scaling functions of road friction and driver, respectively, v and a are the subject vehicle's speed and acceleration, respectively, v_{rel} is the relative speed between the following and the leading vehicles, $a^-_{\max}$ is the maximum deceleration of vehicles, τ is a constant that comprises the driver and system reaction delay, and d_0 is a bias constant.

A piecewise-linear function $f(\cdot)$ can be used for the friction scaling function, and the tire-road friction coefficient μ can be estimated using the wheel slip or wheel speeds. The driver scaling function represents the human neuro delay, and can be bounded for limiting driver influence. Under normal conditions, both scaling functions $f(\cdot)$ and $g(\cdot)$ can be set at one.

Note that the definition of d_w conforms to the model in ISO 15623, which provides the standard evaluation of forward vehicle collision warning systems, whereas the definition of d_{br} is based on the concept of time to collision. The range of I_w, with respect to the relationships among d_r, d_w, and d_{br}, can be presented as the following warning levels:

$$\begin{cases} d_r > d_w \Rightarrow I_w > 1 & \rightarrow \text{safety} \\ d_{br} < d_r < d_w \Rightarrow 0 < I_w < 1 & \rightarrow \text{caution} \\ d_r < d_{br} \Rightarrow I_w < 0 & \rightarrow \text{danger.} \end{cases} \tag{10}$$

This algorithm is used to determine the safe distance in our overtaking maneuver. The first operation involves deciding when the subject vehicle must begin the first lane change into the left lane. In this process, the most dangerous situation is when the vehicle travels into the middle of two lanes, as illustrated in Fig. 5(b). If the relative distance to the lead vehicle is still guaranteed to be safe, the collision during the overall operation of the lane change would not occur. Therefore, the minimum required safe distance d_{safe} can be achieved using (5) as

$$d_{\text{safe}} = I_w d_w + (1 - I_w) d_{br}. \tag{11}$$

According to (10), the value of I_w can be chosen within the range [0, 1]. Note that in this phase, lateral diversion of vehicle motion results in a slight reduction of velocity; such an additional distance is required for the subject vehicle to move to the safe region without colliding with the overtaken vehicle. Recall that the total duration of the lane-change process is $T = 4\Delta_1 + 2\Delta_2$; thus, the travel time required for the vehicle to move to the middle of the two lanes of the road is $T/2$. In this interval of [0, $T/2$], the travel distance of the overtaken vehicle is

$$d_{\text{LV}} = v_{\text{lead}} \frac{T}{2} + \frac{1}{2} a_{\max}^{-} \left(\frac{T}{2} \right)^2 \tag{12}$$

and the travel distance of the subject vehicle is

$$d_{\text{SV}} = v \frac{T}{2} + \frac{1}{2} a_{\max}^{-} \left(\frac{T}{2} \right)^2. \tag{13}$$

The minimum additional distance for beginning the lane-change maneuver without colliding is $d_{\text{SV}} - d_{\text{LV}} = (v - v_{\text{lead}}) \cdot T/2 = v_{\text{rel}} \cdot T/2$. Combined with (11), the safe distance d_{forward} for starting the overtaking operation, namely, from the lane-keeping mode to the lane-change mode, is presented as

$$d_{\text{forward}} = d_{\text{safe}} + v_{\text{rel}} \frac{T}{2}. \tag{14}$$

The next operation involves determining when the subject vehicle must execute the second lane change back to the initial lane. Fig. 5(c) illustrates the process of the second lane-change process, where d_{side} is defined as the safe distance required for the subject vehicle to begin the second lane change after it has completely passed the overtaken vehicle. Determining this distance considers the acceleration of the overtaken vehicle

$$d_{\text{side}} = v_{\text{rel\_side}} T + \frac{1}{2} a_{\text{side}} T^2 \tag{15}$$

where $v_{\text{rel\_side}}$ is the relative speed between the subject vehicle and the side vehicle (overtaken vehicle), and a_{side} is the acceleration of the side vehicle.

For single-vehicle overtaking, the second lane-change starts while the relative distance exceeds d_{side}. As for double-vehicle overtaking, the second lane-change operates under the condition that the relative distances to the side vehicle and the new overtaken vehicle must meet the values of d_{side} and d_{forward} simultaneously. The safe distance d_{forward} with the new overtaken vehicle is the same as (14). If one of the required distances of d_{side} and d_{forward} cannot be satisfied, the system would not activate the second lane change. The main operations of overtaking are described in Appendix A.

The proposed overtaking maneuver focuses not only on the overtaken vehicle in the same lane but also on the side vehicle in the adjacent lane. Moreover, the safe overtaking distance based on the rear-end collision warning algorithm updates continuously so that the speed changes of the vehicles involved in the overtaking operation can be effectively managed. In other words, all vehicles, including other vehicles and the subject vehicle, would not be at risk in the overtaking process.

2) *Reference Speed Generation:* Initially, the reference speed is preset by a human driver. When a slower vehicle is detected ahead, the reference is calculated by the system to follow this vehicle ahead at a safe intervehicular space by adjusting the relative speed. By adopting the constant time-gap spacing policy, this desired spacing varies linearly with vehicle velocity and can be formed as

$$L_{\text{des}} = hv + L_0 \tag{16}$$

where h is referred to as the constant time gap and is usually selected within the range [1, 2.2], and L_0 presets an offset in the desired spacing while the vehicle speed is slow.

The variables for spacing error varies with the velocity and is defined as

$$\delta = d_r - hv. \tag{17}$$

By setting the sliding surface to $S = \delta$ and the control law to $\dot{S} = -\lambda S$, $\lambda > 0$, the desired acceleration of the vehicle based on the constant time-gap policy can be presented as

$$\dot{v} = \frac{1}{h}(\dot{d}_r + \lambda \delta). \tag{18}$$

As inspected using (18), the control policy uses the variation of relative distance and contains an additional term of relative velocity $\dot{d}_r = v_{\text{lead}} - v$ to achieve time headway control. The transfer function associated with the velocity of consecutive vehicles can then be given as

$$G(s) = \frac{V(s)}{V_{\text{lead}}(s)} = \frac{\frac{1}{h}s + \frac{\lambda}{h}}{s^2 + \left(\frac{1}{h} + \lambda \right) s + \frac{\lambda}{h}} \tag{19}$$

where $V(s)$ and $V_{\text{lead}}(s)$ are the Laplace transform of the speed of the subject vehicle $v(t)$ and of the leading vehicle $v_{\text{lead}}(t)$, respectively.

The control law in (16) ensures the condition of string stability:

$$|G(s)|_{s=j\omega} \leq 1, \text{for all } \omega \tag{20}$$

if and only if $\lambda > 0$, which refers to a property that the spacing errors are guaranteed not to amplify as if in a group of vehicles [10], [34]. The other consideration to this control law (18) is the satisfaction of acceptable ride quality, i.e., the comfort of drivers and passengers. The requirement of comfort can be converted to the constraints in that the accelerations and the jerk of a vehicle can be maintained within bounds such as

$$|\dot{v}(t)| \leq \alpha, |\ddot{v}(t)| \leq \beta. \tag{21}$$

To assess this bounding constraint of (21), the transfer function, which presents the relationship from the acceleration of the lead vehicle to the jerk of the subject vehicle, can be given as

$$\Gamma(s) = sG(s) = \frac{s^2 V(s)}{sV_{\text{lead}}(s)} = \frac{s\left(\frac{1}{h}s + \frac{\lambda}{h}\right)}{s^2 + \left(\frac{1}{h} + \lambda\right)s + \frac{\lambda}{h}}. \quad (22)$$

Define the ∞-norm of the transfer function $\Gamma(s)$

$$\|\Gamma(s)\|_\infty = \sup_\omega |\Gamma(j\omega)| \le q. \quad (23)$$

Consequently, it requires that $q \le \beta/\alpha$. The condition for choosing the time gap and the controlling gain can be yielded as

$$\frac{\lambda}{1 + h\lambda} \le \frac{\beta}{\alpha}. \quad (24)$$

This condition imposes a design criterion for the requirement of jerk limitation. Combined with (24), the reference speed strategy from (18) can ensure the string stability while also satisfying the requirement of riding comfort [31], [34].

In the overtaking maneuver, the subject vehicle maintains the preset speed, which is assumed to be higher than the lead vehicle, and performs the first lane-change operation to the adjacent lane. As mentioned in describing the overtaking maneuver, if the second lane change cannot be activated, then the system would track the reference speed that keeps a safe distance L_{des} from the forward vehicle, while providing comfortable driving.

B. Automation Stage

In this stage, the controlling command regarding the speed and steering are calculated by two specific fuzzy controllers, each of which comprises four principle components: a rule base, a decision-making logic, an input fuzzification interface, and an output defuzzification interface. The knowledge of human drivers can be quantified by a set of IF-THEN rules in the rule base, and used as a resource for decision-making logic to apply successive decisions to the current situation. The fuzzification interface takes the crisp inputs and converts them into the fuzzy linguistic terms required in using the decision-making logic. To embody the fuzziness for a particular fuzzy set, membership functions are assigned to the essence of a fuzzy property or operation. Eventually, as required for accurate control, the defuzzification interface converts the conclusions reached by the decision-making logic into crisp control actions. The fuzzy-based controllers are implemented using Mamdani-type rules, as follows, in which both premises and consequences are fuzzy propositions introduced for the steering wheel controller and the speed controller, respectively.

1) *Steering Wheel Controller:* The controller is responsible for the tracking accuracy of the reference trajectories, including straights and curves, as well as riding comfort requirements at all possible vehicle speeds, regardless of environmental uncertainties such as road adhesion, preview errors from the vision system, road curvature variations, sensor noise, and transport lag. The lateral vehicle dynamics with the previewed navigation, which is provided by the vision system mentioned in Section IV-A, is presented using the following linear system [16]:

$$\dot{x} = \begin{bmatrix} a_1 & a_2 & 0 & 0 \\ a_3 & a_4 & 0 & 0 \\ 1 & L_d & 0 & v \\ 0 & 1 & 0 & 0 \end{bmatrix} x + \begin{bmatrix} b_1 \\ b_2 \\ 0 \\ 0 \end{bmatrix} \delta_f + \begin{bmatrix} 0 \\ 0 \\ 0 \\ -v \end{bmatrix} \rho_{Ld} \quad (25)$$

where the state vector $x = [v_y, r, y_{Ld}, \varepsilon_{Ld}]^T$, and v_y and r are the lateral velocity (m/s) and yaw rate (rad/s), respectively, y_{Ld} and ε_{Ld} are the measured lateral offset (m) to the lane center and the yaw angle (rad) between the lane tangent and the vehicle axis at a look-ahead distance L_d (m), respectively, the control input δ_f is the angle (rad) of the front wheel of the vehicle, and the road curvature ρ_{Ld} (1/m) is viewed as an exogenous disturbance.

The upper-half equations of (25) present the yaw motion of a front-steering vehicle and are the so-called bicycle model with two degrees of freedom [16], [35], which are represented by the variation of lateral displacement and yaw angle. The parameters of the bicycle model (25) are determined using

$$\begin{aligned} &a_1 = -(C_f + C_r)/Mv\ ,\ \ a_2 = (bC_r - aC_f)/Mv - v \\ &a_3 = (bC_r - aC_f)/I_z v\ ,\ \ a_4 = (b^2 C_r - a^2 C_f)/I_z v \\ &b_1 = C_f/M, b_2 = aC_f/I_z \end{aligned} \quad (26)$$

where a and b are the distance (m) from the front and rear axle to the center of gravity (CG) of the vehicle, v is the longitudinal velocity (m/s) of the vehicle, C_f and C_r are the lateral tire stiffness coefficients (Nt/rad) of the front and rear tires, respectively, M is the mass of the vehicle, and I_z is the moment of inertia around the CG.

The control objective in the lane-keeping maneuver involves regulating the previewed lateral offset y_{Ld} at zero. Given the vehicle model (25), the state feedback control appears to be naturally applied and given as $\delta_f = -K_{fb}x$. The controller K_{fb} can be computed using an H_∞ optimization as follows:

$$K^*_{fb} = \arg\min_{K_{fb}} ||T_{\rho_{Ld} \to y_{Ld}}||_\infty \quad (27)$$

where $T_{\rho_{Ld} \to y_{Ld}}$ presents the transfer function from ρ_{Ld} to y_{Ld}. Notably, the feedback control should be designed under the highest speed v of interest and a preconsidered transport lag, such that stability at lower speeds and riding comfort can be guaranteed [16].

As for the lane-change maneuver, the reference trajectory regarding the lateral offset signal y_{des}, which is calculated in the data fusion stage, is fed into the feedback of y_{Ld} and ε_{Ld} such that the generation of steering control can execute the lane-change operation. That is, the lane-change command of steering wheel control is

$$\begin{aligned} &\delta_f(t) = -K_{fb}(x(t_0) \pm x_{\text{LC}}(t)), \quad t \in [t_0,\ t_0 + T] \\ &\text{with} \quad x_{\text{LC}} = \begin{bmatrix} v_y & r & y_{\text{des}} & y_{\text{des}}/L_d \end{bmatrix}^T \end{aligned} \quad (28)$$

where t_0 represents the time at which the system switches from the lane-keeping to the lane-change operation, T represents the total duration of the aforementioned lane change, and $\pm$ represents the direction of the lane-change maneuver.

Remark: As in (28), lane-change operation is considered an open-loop lane-change maneuver regarding the steering command, which contains the closed-loop lane-keeping control. When beginning the lane-change process, the lateral velocity and yaw rate are converged to zero, whereas the previewed lateral offset of the vehicle can be regulated to the desired value of y_{des}. At the end of the lane-change maneuver, the vehicle returns to lane-keeping operation to track the centerline of the adjacent lane.

Although the static feedback control strategy suffices to meet the requirements of vehicle lateral control, it is sensitive to the parameters of the system. Furthermore, the desire to steer the vehicle in a more human fashion motivates the adoption of a fuzzy adaptive scheme as part of the lateral control design strategy. Human driving knowledge can be factored into deriving the behavior response of vehicle steering. A scheme of fuzzy gain scheduling (FGS) based on the fuzzy set theory is proposed herein to auto-tune the feedback control. The essential part of the proposed FGS is the inference rule base, which constitutes engineering judgment and driver knowledge. The inference rule base supports more human-like driving behavior during the process of maintaining the reference trajectory, i.e., humans usually drive more aggressively at low speeds and more gently at high speeds, even when the deviation between the vehicle and the centerline of the road is large. Accordingly, the linguistic input variables are the immediate speed of the vehicle and lateral offset from the centerline at the look-ahead distance. FGS yields the proper tuning gain, based on the following rules:

$$i\text{th rule : IF } v \text{ is } \tilde{A} \text{ and } |y_{Ld}| \text{ is } \tilde{B},\ \text{THEN } \Delta_{\delta i} \text{ is } \tilde{C} \tag{29}$$

where $\tilde{A}$, $\tilde{B}$, and $\tilde{C}$ are corresponding linguistic terms

$$\begin{aligned} \tilde{A} &= \{\text{LOW}, \text{MED}, \text{HIGH}\} \\ \tilde{B} &= \{\text{LB}, \text{LS}, \text{ZO}\} \\ \tilde{C} &= \{S,\ M,\ L\} \end{aligned} \tag{30}$$

where the notations are LOW = low speed, MED = medium speed, HIGH = high speed, LB = lateral big, LS = lateral small, ZO = zero, S = small, M = medium, and L = large.

Table I shows the rule base of FGS. These parameters of the membership functions for prior and consequent expressions are tuned manually to ensure satisfactory driving behavior. The shapes chosen in FGS are trapezoidal for v and triangular for $|y_{Ld}|$ and Δ_δ, as shown in Fig. 6. In the defuzzification strategy, the center-of-area (COA) method is adopted to determine the gain

$$\Delta_\delta = \sum_{i=1}^{9} \mu_i \cdot \Delta_{\delta i} \Big/ \sum_{i=1}^{9} \mu_i \tag{31}$$

where $\Delta_{\delta i}$ represents the consequence of rule μ_i and is a weighting parameter calculated from the membership operation based on

$$\mu_i = \min\left(\mu_A(v),\ \mu_B(|y_{Ld}|)\right) \tag{32}$$

where μ_A and μ_B represent the membership function of input v and input $|y_{Ld}|$, respectively.

TABLE I
RULE BASE OF FGS

v / $\lvert y_{Ld}\rvert$	LOW	MED	HIGH
LB	*L*	*L*	*M*
LS	*L*	*M*	*S*
ZO	*M*	*S*	*S*

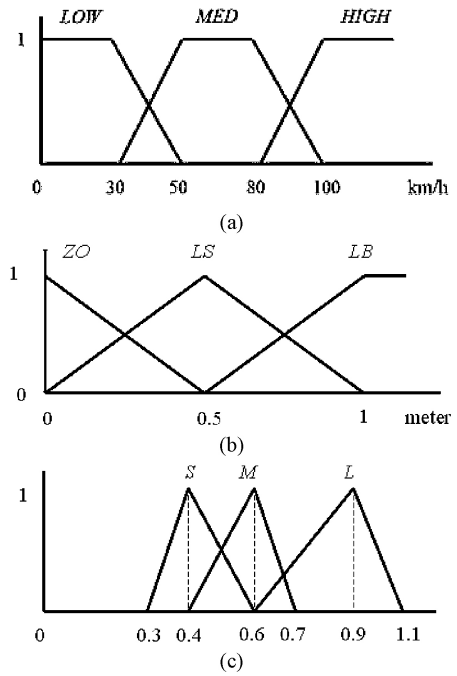

Fig. 6. Membership functions for (a) vehicle speed v, (b) absolute lateral offset at the look-ahead distance $|y_{Ld}|$, and (c) FGS-based adaptive gain Δ_{fg}.

The terminal quantity of the steering wheel controller is tuned using FGS, $\delta_{\text{SW}} = \Delta_\delta \delta_f$. The principle of the crossover model can be applied to examine the utility of FGS. The analysis results that reveal the evidence of the crossover model principle for the FGS-compensated feedback controller can be compared to the results in [16]. Note that FGS aims to adjust the quantity of feedback control, and the membership functions of $\tilde{C} = \{S, M, L\}$ should, therefore, be designed carefully such that the system (25) is not destabilized with the highest vehicle velocity. Appendix B summarizes the design result that can be useful for system stability analysis associated with FGS.

2) *Speed Controller:* An ordinary driver can control the throttle and brake systems easily to reach the desired speed, even when using different types of engine, automatic transmission in the gear box, and brake system in each vehicle. Hence, the design concept of throttle or brake actuation originates from human-driving behavior. Adopting the fuzzy logic-based control methods to replace the classic dynamic model and importing the human driving experience into fuzzy rule not

only avoid the difficulty for control design (based on such a complicated mathematical model) but also allow the system to simulate humanlike driving behavior [15], [27].

The fuzzy inputs are chosen as the speed error, which is the difference between the current speed and those of the reference speed and its derivative $(e,\ \dot{e})$. If we set five membership functions for each variable, then 25 fuzzy rules would be in the entire fuzzy rule table. A drawback would result from building many fuzzy rules, thereby increasing the computation load for the implementation loop. Conventionally, a lookup table is used to approximate a fuzzy rule table in programming. However, the method not only requires more storage space on the memory of the device but also causes discontinuous outputs that worsen the controlling performance of the original FLC. Therefore, a proportional-derivative (PD)-based single-input fuzzy logic control (SFLC) is employed in the speed regulation design. For conventional FLCs, the fuzzy rule base is constructed in a 2-D space for using the error and error change phase plane. Most 2-D fuzzy rule bases have the so-called skew-symmetric property [36]. Thus, given $e = v - v_{\text{des}}$ and $\dot{e} = a - a_{\text{des}}$, the switching line that represents the main hyperplane of the 2-D fuzzy rule table can be defined as a sliding manifold

$$S = \dot{e} + \alpha_s e \tag{33}$$

with the slope α_s, which determines the convergence rate to the origin when the sliding mode occurs.

The original fuzzy inputs of the error and error change can be replaced by one signed distance D, which is defined as the perpendicular distance from an operating point to the projection point on the switching line S. This new fuzzy input of the signed distance can be calculated as

$$D_s = \text{sgn}(S) \cdot D = \text{sgn}(S) \cdot \frac{|\dot{e} + \alpha_s e|}{\sqrt{1+\alpha_s^2}} = \frac{\dot{e} + \alpha_s e}{\sqrt{1+\alpha_s^2}} \tag{34}$$

with

$$\text{sgn}(S) = \begin{cases} 1, & \text{for } S > 0 \\ -1, & \text{for } S \le 0 \end{cases}$$

The new fuzzy input D_s involves speed error and error change with a proportional gain and a derivative gain, i.e., $D_s = k_p e + k_d \dot{e}$ with $k_p = \alpha_s \Big/ \sqrt{1+\alpha_s^2}$ and $k_d = 1 \Big/ \sqrt{1+\alpha_s^2}$. The term of speed error can adjust the throttle or brake degree when the speed is not at the reference, whereas the term of error change can smooth the actuation command in the exact manner as the damping effect. The associated fuzzy rule form is

$$R_k : \text{IF } D_s \text{ is LD, THEN } u \text{ is LU} \tag{35}$$

where LD and LU are the linguistic term sets for the fuzzy input and the fuzzy output, respectively

$$\begin{aligned} \text{LD} &= \{\text{NB, NS, ZO, PS, PB}\} \\ \text{LU} &= \{\text{NB}u, \text{NS}u, \text{ZO}u, \text{PS}u, \text{PB}u\} \end{aligned} \tag{36}$$

where the notations are NB = negative big, NS = negative small, ZO = zero, PS = positive small, PB = positive big, NBu = negative big controlling, NSu = negative small controlling, ZOu = zero controlling, PSu = positive small controlling, and PBu = positive big controlling.

TABLE II
RULE BASE OF SFLC

D_s	NB	NS	ZO	PS	PB
u	NBu	NSu	ZOu	PSu	PBu

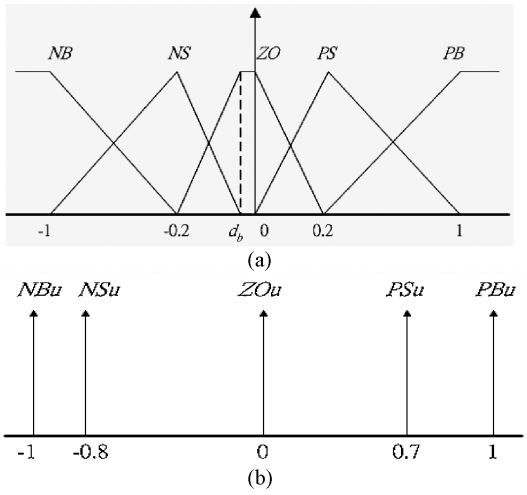

Fig. 7. Membership functions of (a) fuzzy input D_s and (b) controlling degree u.

Table II lists the fuzzy rule table, and the membership functions for the fuzzy input and output are illustrated in Fig. 7. The total number of fuzzy rules for the speed controller is only five, which is much fewer than the 25 fuzzy rules of the 2-D fuzzy control, such that generating and tuning rules are much easier. The output membership functions are defined as five singletons, which, after defuzzification, generate a crisp value of u in $[-1, 1]$. In the defuzzification operation, the CG method for the crisp consequence of each rule is applied as

$$u = \sum_k^5 \mu_k(D_s) \cdot u_k \Big/ \sum_k^5 \mu_k(D_s) \tag{37}$$

where μ_k represents the weight of the kth rule and u_k is the value of the output inferred using the kth rule.

The center of the membership function of the fuzzy output, LU ={NBu, NSu, ZOu, PSu, PBu}, should be selected to satisfy the condition of closed-loop system stability, as summarized in Appendix C.

Remark: The output value indicates the controlling degree that remains positive regarding acceleration of the throttle driver, but is negative regarding deceleration of the brake motor. In this manner, the actions of the throttle and brake are not executed simultaneously. Note that the offset d_b in the "ZO" membership function represents the reachable deceleration when the brake pedal is released because of the rolling resistance of the tire and road as well as the engine inertia. If the required deceleration is extremely high (i.e., $D_s < d_b$), then the brake control is activated. This offset also assures that the throttle is completely released before the brake starts to activate.

Fig. 8. eZdspF2812 board.

TABLE III
PARAMETERS OF THE VEHICLE AND CONTROL SYSTEM

Description		Value
M	Vehicle mass	1940 kg
I_z	Moment of inertia	3673 kg·m^2
C_f	Lateral stiffness coefficient of front tires	131 391 Nt/rad
C_r	Lateral stiffness coefficient of rear tires	115 669 Nt/rad
a	Distance from front axle to the CG of vehicle	1.193 m
b	Distance from rear axle to the CG of vehicle	1.587 m
W	Road width	2.5–3.5 m
T	Period for lane-change process	4.2–5.8 s
$a_{\max}^{-}$	Maximum deceleration of vehicle	6 m/s^2
τ	Reaction delay from human and system	0.6 s
d_0	Bias of the warning distance (8)	4 m
α	Bounded acceleration	2 m/s^2
β	Bounded jerk	3 m/s^3
L_0	Offset in the desired spacing	2 m
h	Time gap	1 s
λ	Controlling gain of (18)	1.2
L_d	Look-ahead distance	10 m
α_s	Slope of main hyperplane of SFLC	1.5

V. IMPLEMENTATION ON AN EMBEDDED DSP PLATFORM

The proposed system was implemented as a low-cost real-time embedded computing system and installed on a testbed vehicle. This real-time experimental system is ported and evaluated on a TI TMS320F2812 embedded DSP platform, named eZdspF2812, as shown in Fig. 8. This DSP platform is operated on a 150-MHz clock rate with on-chip 18K RAM, up to 128 K × 16 Flash ROM, 16 channels of 12-b A/D converters, and 56-b general-purpose input/output (I/O). Hence, it can provide both the advantages of the efficiency of multiple digital-motors control implementation as well as the capability of real-time signal processing for complex algorithms, such as the data fusion and fuzzy control computations applied in our proposed system.

Table III lists the crucial parameters and associated values of the vehicle platform and proposed system. The development tool is the code composer studio (CCS) provided by TI, and the program can be loaded into the DSP, a real-time environment that also includes the communication peripheral that drivers require for accessing the sensors and actuators equipped in the vehicle. An event manager in the CCS allows the definition and application of numerous time-triggered, preemptions of software modules, following a fixed priority scheme [37]. In our system, among such modules are the reference trajectory and reference speed generation, fuzzy controllers of steering, throttle and braking actuation, as well as low-level PID motor controllers. Fixed-point data formats are employed by the C-code to maximize the accuracy and minimize the code size and computation times of the program. Numerical errors must be avoided because of the truncation, rounding, and overflow of numerical data. In this real-time experimental environment, the high-level control algorithms are relieved of the task of synchronizing the read and write processes among different devices.

Implementing fuzzy controllers frequently requires large amounts of multiplication and division instructions demanding high accuracy. Moreover, implementing fuzzy controllers on a DSP raises two main concerns: the processing duration for computing the output of fuzzy controllers and the amount of memory used. The former problem can be solved using triangular and trapezoidal membership functions, as illustrated in Figs. 6 and 7. In this situation, a maximum of four rules are effective at any time; thus, only four centers and four membership degrees must be calculated in the defuzzification strategy. In calculating the outputs in (30) and (35), multilinear expressions regarding only addition and multiplication operations are preferred. Therefore, the membership functions in Figs. 6 and 7 are normalized as linear functions to represent linguistic labels by an interpolation-type rule base. The inference operators, such as the linguistic "and," are used as products, and the constant values are employed for each rule's consequent part.

The computation time and code size of the fuzzy controller can also be reduced using the PD-like SFLC, as described in the previous section, while maintaining nearly the same performance as that of the original FLC. The proportional gain and the derivative gain in (33) can be calculated beforehand, and the numbers of the fuzzy rule are greatly reduced, causing significant mitigation of computational complexity, particularly when the rule base is large.

The algorithms in the data fusion and automation stage, as well as the low-level PID controllers, can be transformed into the discrete-time domain using the backward Euler integration method. Other algorithms are proceeded using a series of scalar multiplication and addition instructions. The TI TMS320F2812 DSP is optimized to implement digital filters because it has distinctive internal structures to multiply a number by a constant and add the previous product following a single instruction. Hence, the result is a DSP-based implementation in real time used as a straightforward approach for linear combination of the controller. Furthermore, numerous platform-based optimization techniques combing C and various assembly programs can be used to improve the DSP hardware performance. Although the C compiler of TI has sophisticated optimization capabilities, programs such as bit-reverse, parallel threads processing, and A/D conversion with an ordinary C code may still demonstrate insufficient performance. The solution regarding this problem involves substituting them with inline assembly codes. In this paper, the DSP Library (DSPLIB) provided by TI was adopted to increase the computational efficiency [30].

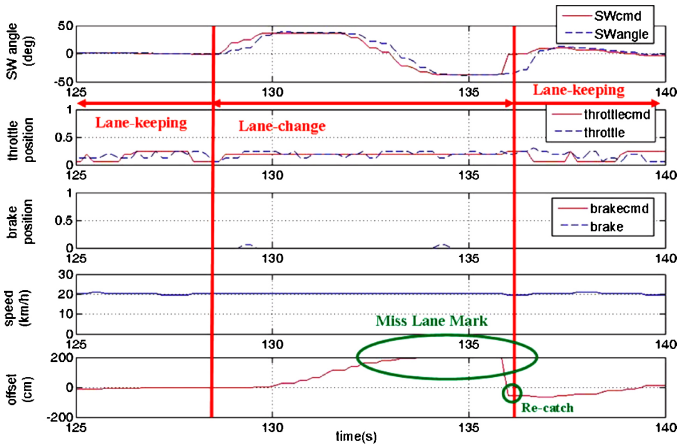

Fig. 9. Performance results of the combined lane-keeping and lane-change operations.

The eZdsp board offers a direct interface of the IEEE 1149.1 JTAG controller and emulation connector, which is used as a communication link to an external laptop. The development program can be modified from this laptop, and during the experimental operation, the data of the system response can be collected. Using the software optimization, the average computation times of the data fusion stage and automation stage are 13 and 22 ms, respectively. The control loop in our system was set at 50 ms in our experiments. In each computing period, the DSP processes the proposed algorithms from sensor data preprocessing to the data fusion stage, and then to the automation stage. The DSP then outputs the new controlling for the motor drivers of the steering wheel, throttle, and brake. The low computation costs ensure that the proposed system can effectively satisfy the demand of human reaction time in driving tasks (as revealed in [38]).

VI. Experimental Results

Our implemented system is a low-cost DSP-based system, which is installed in a vehicle by conducting various tests of real-road environments. The experimental results of the combined lane keeping and lane changing are initially introduced. The overtaking maneuver demonstrations include two three-car scenarios. The subject vehicle is driven by the proposed system, and other vehicles are manually driven. Because human driving behavior is unpredictable, the flexibility of the developed system can be demonstrated. In addition to the experimental results, some possible bottleneck issues, which may result in the limitation of the vehicle speeds for our system, are also discussed.

A. Combined Lane-Keeping and Lane-Change Maneuver

The performance results of the combined lane-keeping and lane-change operations at the speed of 20 km/h are shown in Fig. 9. The lane-keeping mode switched to lane-changing mode at 128 s. During the period of the lane-changing process (from 128 to 137 s), the reference trajectory is substituted by a virtual lateral offset profile, which is generated by the specified lateral jerk. The previewed lateral offset increases because the vehicle is steered to the left boundary of the lane. The lane mark data cannot be recognized by the vision system in the lane-to-lane transition, and the lateral offset holds the value of 200 cm. Notably, we designed this switch from the lane change to the beginning of the lane-keeping operation when the lane mark data of the left lane are immediately detected by the vision system. This result can be observed in the fourth frame (offset) in Fig. 9 at 136 s. Thus, the period of the eventual lane-change maneuver is shortened, allowing the lane-keeping maneuver to lead the subject vehicle and align itself to the target centerline, i.e., the vehicle is moving in the left lane and the lane mark can be detected again by the vision system so the system can proceed to the lane-keeping operation.

B. Overtaking Maneuver for Three-Car Experiment

The experimental scenarios can be divided into two circumstances. The difference is that the condition for the second lane-change activation, which relies on the relative distances to the front vehicle and the side vehicle, must satisfy the values of d_{forward} and d_{side}. If one of them cannot meet, the second lane change is not activated and the speed of the subject vehicle is reduced to maintain a safe headway from the front vehicle to avoid a crash. Accordingly, the overtaking maneuver for three cars includes the circumstance of a double lane change and single lane change, respectively.

The two front vehicles were manually driven to test the system against the human driving actions in other vehicles. At the beginning of the experiment, the two front vehicles traveled at a speed of approximately 15 km/h and the subject vehicle traveled at 20 km/h. Figs. 10(a) and 11(a) show the frame sequences and the trajectories of the double-overtaking and the single-overtaking processes, respectively. The first lane-change process is identical to the task involved in the overtaking maneuver in the two-car scenario. As shown in Figs. 10(b) and 11(b), the first lane change begins when the relative distance (solid line) to the overtaken vehicle reaches the value of d_{forward} (dashed line). After the first lane change was completed, the lane-keeping operation in the adjacent lane continued. Under the circumstance of double overtaking, as shown in Fig. 10, the reference speed for the lane-keeping operation was increased to 30 km/h. This speed allowed the subject vehicle to pass the overtaken vehicle more quickly. As shown in Fig. 10(b), although the relative distance to the new overtaken vehicle satisfies the value of d_{forward}, the second lane change was executed until the relative distance to the side car (previously overtaken vehicle) reached the distance d_{side} at 69 s. The absence of oscillations in the trajectory plots of the subject vehicle indicates smooth driving mode changes.

Under the circumstance of single overtaking, as shown in Fig. 11, the subject vehicle completed the first lane change at 44 s. Although the relative distance to the new overtaken vehicle satisfied d_{forward}, the distance to the side vehicle was inadequate to perform the second lane change. Although the relative distance met the value of d_{side} at 65 s, the distance to the overtaken vehicle was not adequate to return to the right lane. The subject vehicle reduced its speed to maintain a safe distance of 12 m from the front vehicle. As shown in the speed plot of Fig. 11(b), the speed of the subject vehicle eventually

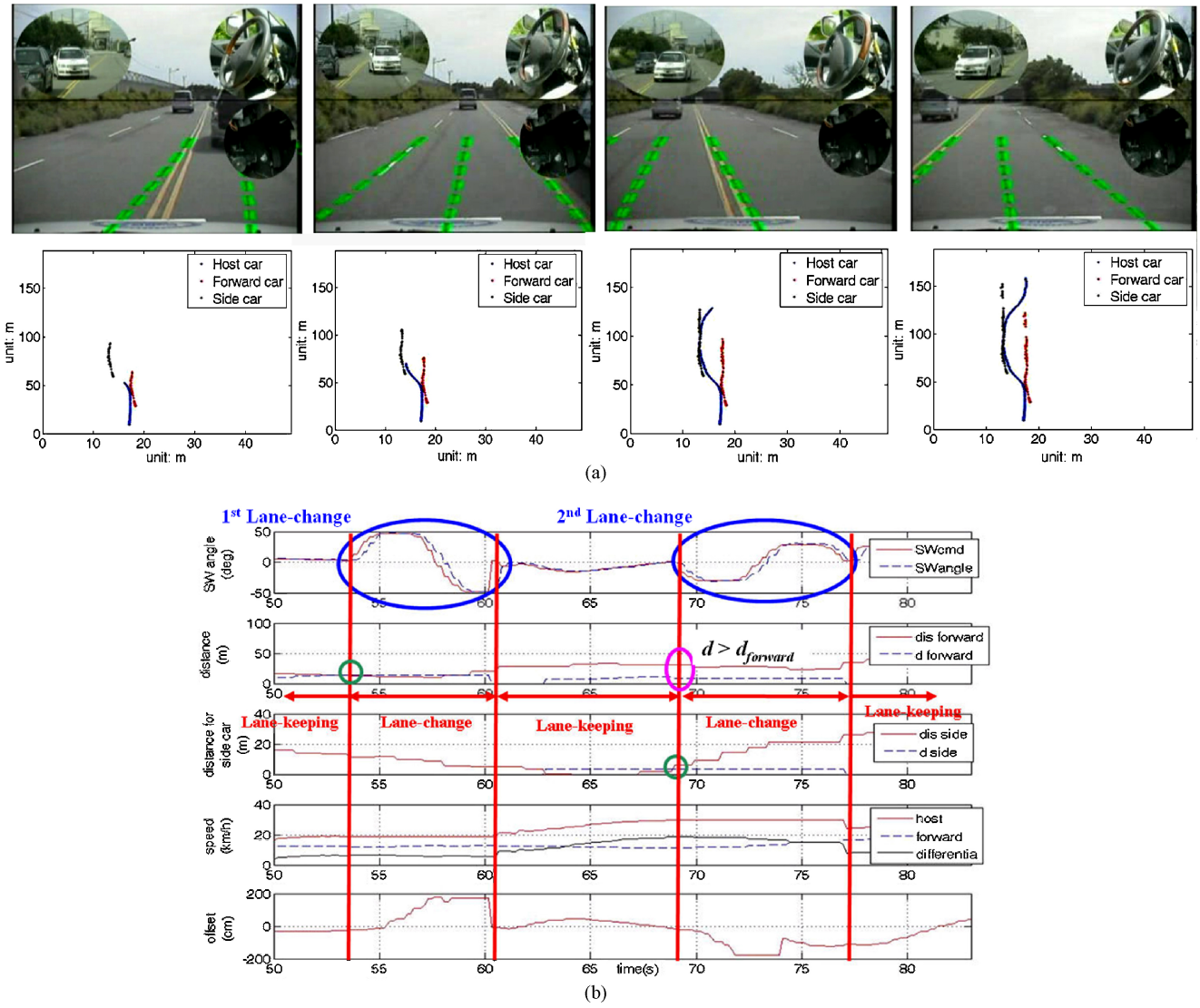

Fig. 10. (a) Sequential images for the double-overtaking scenario in the three-car experiment. The top image was captured from the vision system, the top-left subimage was captured from the video on the side car, and the top-right subimages display the automation of the steering wheel, throttle, and brake pedal, respectively. The lower graph represents the trajectory of three vehicles during this experiment. (b) Performance results of the double-overtaking operation for three-car experiment.

matched the front vehicle at approximately 18 km/h. In this experiment, the overtaking performance was also consistent with the control system design, i.e., unless the two distances conformed to d_{forward} and d_{side} simultaneously, the second lane change would have activated.

Fig. 12 shows the results of a double-overtaking experiment with higher speed on the freeway. The overtaken vehicle was driven ahead at a speed of approximately 60 km/h. The overtaking vehicle was set at a reference speed of 70 km/h to detect the slower preceding vehicle. Again, the first phase of the overtaking maneuver was activated when the relative distance reached the value of d_{forward}. After detecting the preceding vehicle in the adjacent lane, the overtaking vehicle slightly decreased its reference speed to maintain a safe distance and performed lane keeping. The second phase of the overtaking maneuver was enabled until the two distance conditions were satisfied at 51 s. Finally, the overtaking vehicle returned to the original lane and continued onward.

Table IV summarizes our test results, including low and high speeds, under different traffic conditions of various environmental vehicles (including overtaken and side vehicles). Notably, the duration of the lane-change process mainly depends on the redetection speed of lane marking information from the vision system. In addition, the average time required for this process is approximately 5 s, which is consistent with the calculation of the total duration of the lane-change process T (as described in Section IV-A). Sets A, B, and C indicate that the system can efficiently detect the overtaken vehicle either in moving or stationary actions, and can promptly perform a safe overtaking maneuver by applying the proposed algorithms. Based on Sets D, E, and F, the second lane change is conducted appropriately until the distance of the subject vehicle to the overtaken vehicle achieves the condition of (15). Once the overtaking maneuver has been completed, the subject vehicle performs lane keeping at the reset reference speed. All of the trials satisfy the design requirements, demonstrating that the

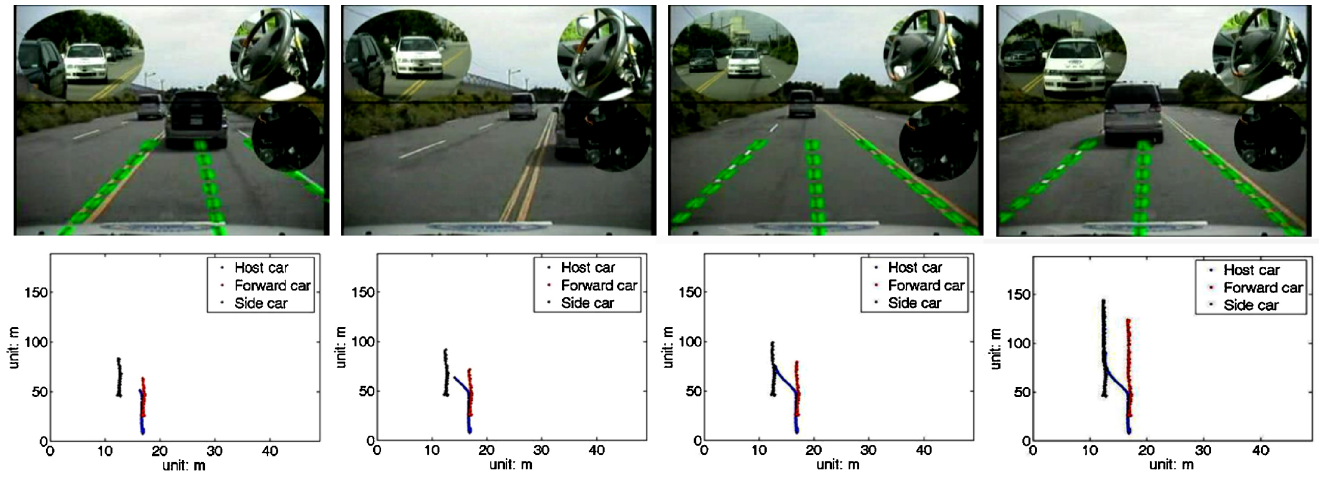

(a)

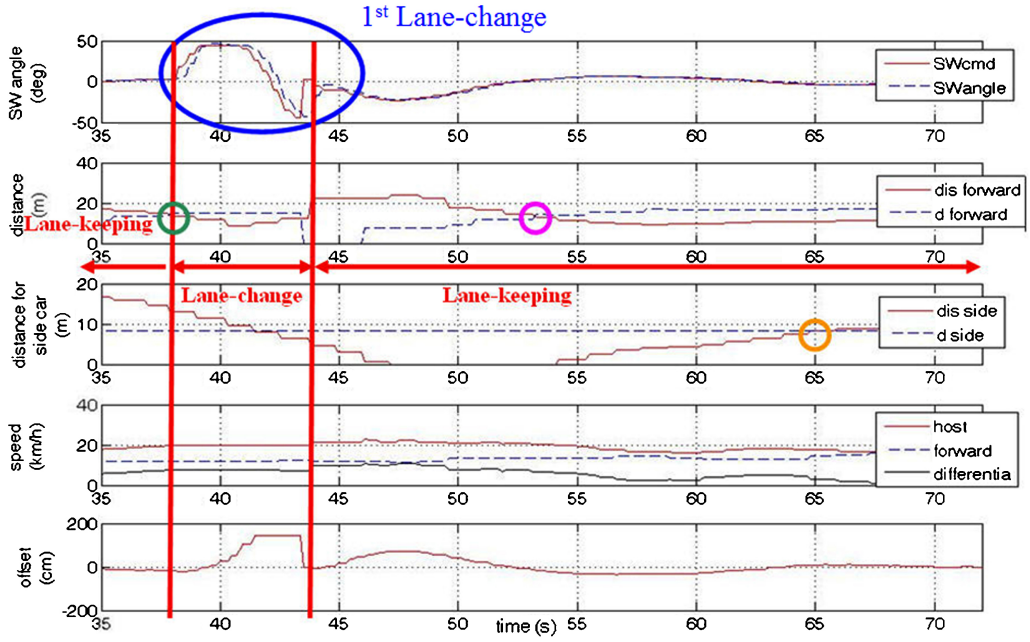

(b)

Fig. 11. (a) Sequential images of the single-overtaking scenario in the three-car experiment. The top image was captured from the vision system, the top-left subimage was captured from the video on the side car, and the top-right subimages display the automation of the steering wheel, throttle, and brake pedal, respectively. The lower graph represents the trajectory of the three vehicles during this experiment. (b) Performance results of the single-overtaking operation in the three-car experiment.

developed system is capable of performing overtaking maneuvers with adequate safety regarding neighboring vehicles.

C. Bottleneck Analysis

In the presented driver-assistance system, multiple sensors and actuators are integrated with the DSP-based embedded system to perform various operations for achieving the overtaking maneuver. There exists some bottlenecks that constraint the system performance in the maximum speed of the subject vehicle. Therefore, it is of interest to investigate system bottlenecks and how they react to an increased driving speed while maintaining the overall system reliability and stability.

From the results of Table IV, the operation period of lane change is about 5 s either at low speed 30 km/h or at high speed 70 km/h, and within this time period, the ride comfort can be preserved. However, the distance traveled in 5 s at these two speeds is significantly different. Recall that our lane-change maneuver is an open-loop control strategy and its feasibility can be easily declined by changes in road curvature and level. This bottleneck thus limits the maximum speed in performing the overtaking maneuver. The possible solution to this bottleneck can design augmented estimators to further supplement the vehicle current position and future path prediction [39]. However, this technique is computationally demanding for the embedded processor operated at 150 MHz with limited computation power, because of large numbers of matrix computations in the real-time implementation.

The other bottlenecks come from the hardware limitations of our utilized facilities, such as the vision system, motor drivers, and the V-V communication device. Although real-

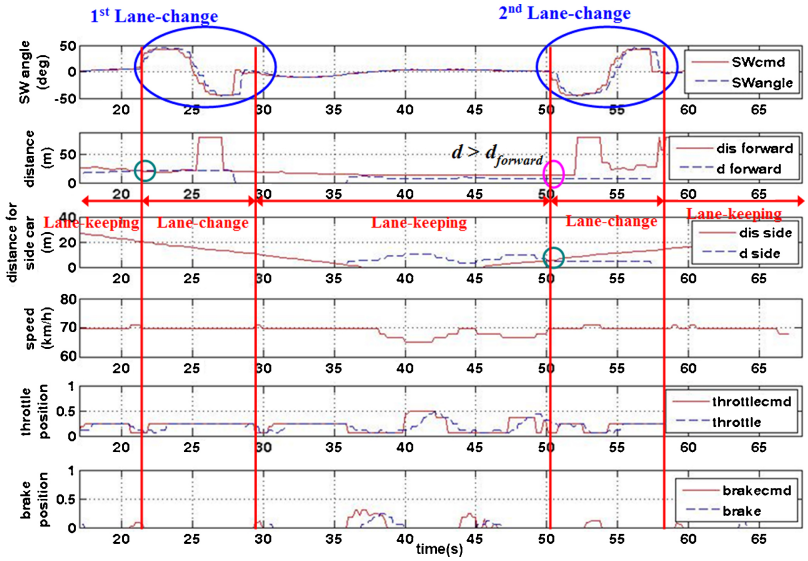

Fig. 12. Performance results of the double-overtaking operation in three-car experiment.

TABLE IV
TEST RESULTS UNDER DIFFERENT ON-ROAD TRAFFIC CONDITIONS

Test Set	Set Descriptions	System Performing	Processing Results
Set A	The speed of the subject vehicle is set as 30 km/h; the overtaken vehicle is moving at approximately 20 km/h; no side vehicle is included.	Double-overtaking operation	Complete overtaking maneuver takes approximately 22 s. (First LC takes approximately 4.7 s, LK at the speed 30 km/h takes approximately 11.8 s, and the second LC takes approximately 5.5 s).
Set B	The speed of the subject vehicle is set as 30 km/h; the overtaken vehicle stops at 20 m ahead; no side vehicle is included.	Double-overtaking operation	Complete overtaking maneuver takes approximately 12 s. (First LC takes approximately 5.1 s, LK at the speed 30 km/h takes approximately 1.9 s, and the second LC takes approximately 4.9 s.)
Set C	The speed of the subject vehicle is set as 70 km/h; the overtaken vehicle is moving at approximately 60 km/h; no side vehicle is included.	Double-overtaking operation	Complete overtaking maneuver takes approximately 31 s. (First LC takes approximately 5.2 s, LK at the speed 70 km/h takes approximately 20 s, and the second LC takes approximately 5.8 s.)
Set D	The speed of the subject vehicle is set as 30 km/h; both the overtaken vehicle and the side vehicle are driven at approximately 20 km/h, and the distance between them is kept approximately 10 m.	Single-overtaking operation	Only the first LC is complete and takes approximately 4.8 s. The subject vehicle decelerates to the speed approximately 20 km/h and follows the side vehicle.
Set E	The speed of the subject vehicle is set as 30 km/h; the overtaken vehicle stops at 20 m ahead; the side vehicle is driven at approximately 20 km/h.	Double-overtaking operation	Complete overtaking maneuver takes approximately 28 s. (First LC takes approximately 5.2 s, LK at the speed 30 km/h takes approximately 18.2 s, and the second LC takes approximately 4.9 s.)
Set F	The speed for the subject vehicle is set as 70 km/h; both the overtaken vehicle and the side vehicle are manually driven at approximately 60 km/h, and the distance between them is kept approximately 30 m.	Double-overtaking operation	Complete overtaking maneuver takes approximately 35 s. (First LC takes approximately 5.6 s, LK at the speed 70 km/h takes approximately 23 s, and the second LC takes approximately 5.7 s.)

LC: lane change. LK: lane keeping.

time ability can be achieved by our vision system, the effective look-ahead distance is limited within 10 m (in Table III) due to the restricted image resolution. In addition, the transport lag from the control system to the actuation motors is about 0.6 s (as the reaction delay in Table III). This kind of bottleneck limits the highest lane-keeping speed to 80 km/h in tortuous roads that will induce more disturbances to the lateral vehicle dynamics. In order to achieve cooperative safety, our overtaking maneuver applies wireless communications to communicate with the neighboring vehicle and the V-V data from other vehicles is at 10 Hz. The accuracy and the transmission latency of V-V communications are directly related to the reliability of our system and thus the vehicle driving speed must also account for this bottleneck.

VII. CONCLUSION AND DISCUSSION

This paper presented a DSP-based driver-assistance system capable of performing driving maneuvers, such as lane-keeping, lane-changing, and overtaking with a set of safety and comfort considerations. The overall system was installed in a commercial vehicle to verify our designed system,

which was constructed in a hierarchical autonomy structure, achieving integrated speed and steering control. The data fusion stage determined the reference speed and the reference lateral trajectory among various situational assessments. The automation stage was designed based on the fuzzy control technique for managing vehicle actuators (i.e., the steering wheel, throttle, and brake pedals) in a manner that mimics the driving task of humans. In addition to theoretical substantiation, our system, combined with multiple sensors and abundant equipment installed in a real vehicle, was demonstrated to assess the less conservative safety of the overtaking maneuver under three-car circumstances, without endangering any of the vehicles involved in the process.

In the current system, installing the vision system, range finder, and communication between vehicles emphasized the benefit of increasing the safety of overtaking maneuver cooperatively. Because the presented system mainly focused on providing comfort and safety assistance for overtaking maneuvers, some critical situations such as emergent overtaking behaviors and sharp curves may not be applicably based on our approach. Including the dynamic positioning data and speed of the neighboring vehicle could improve this work further and enhance the reliability of our system. Furthermore, the reliability of the system should account for the act of driving concerning oncoming traffic data, using a vision-based computing module in the control loop, particularly regarding the short latency in response to critical situations. Formulating the cost function and assignment used in tactical-level reasoning is difficult. A feasible solution may involve employing a learning-based approach for continually refining the system's parameters to achieve the characteristics of human control. To resolve some bottleneck issues mentioned in Section VI-C, some high-end embedded DSP platforms with higher computation resources, which can provide a more computation-intensive ability and a complementary combination of the ARM processor, can be used to provide a best-fit solution for advancing our system with the embedded operating system, graphical user interface module, and peripheral I/O control facilities. Finally, for some vehicles that do not have communication capability, the intelligent arbitration and application logic are required for safety applications in multiple cooperative and noncooperative driving environments.

APPENDIX A
OPERATION OF OVERTAKING MANEUVER

The main operations of overtaking are described in Algorithm 1.

Algorithm 1: Overtaking (OT): Estimate the overtaking distance for determining the time to switch between lane keeping (LK) and lane changing (LC)

```
Input: road width W, headway distanceA (with respect to the
forward vehicle), headway distanceB (with respect to the side
vehicle), velocity.
Output overtaking distance d_forward, d_side
while flagOT do
    /* flagOT is true for starting OT, the default is LK */
    distanceA = GetDistance()
    /* obtain the headway distance by the laser range finder*/
    d_forward = GetForwardDis()
    /* calculate the safe distance for starting OT */
    if (distanceA == d_forward) then
        /* check the headway distance to be safe for OT */
        T = GetLCtime(W)/* calculate the total time for the
        first LC */
        flagLC_1 = 1 /* execute the first LC (to left lane) */
        if (flagLC_1 == 1) then
            distanceA = GetDistance()
            distanceB = GetSideDistance() /* obtain the
            distance with respected to the front and
            the overtaken vehicle */
            if (distanceB ==0) then
                /* check whether the subject vehicle has
                overtaken the
                overtaken vehicle*/
                Passflag = 1
                if (Passflag ==1) then
                    d_forward = GetForwardDis()
                    d_side = GetSideDis()
                    /* calculate the two safe distances for the
                    second LC */
                    if (distanceA >= d_forward) and
                    (distanceB >= d_side) then
                        /* check these two distances to be
                        safe for OT */
                        dir = -dir /* change the LC direction
                        */
                        T = GetLCtime(W)
                        /* calculate the total time for the
                        second LC*/
                        flagLC_2 = 1
                        /* execute the second LC to return to
                        the original lane */
                        else
                        v_des = GetVelocity()
                        /* calculate the safe speed for
                        following
                        the new lead vehicle */
    flagOT =0        /* change to LK */
```

APPENDIX B
STABILITY CONSIDERATION OF FGS-COMPENSATED STATE FEEDBACK CONTROL DESIGN

By considering the state space form of (25) at the extremes of velocity $v_{\max}$ as

$$\dot{x} = A(v_{\max})x + Bu \tag{B1}$$

and the controlling input $u = \delta_{SW} = \Delta_\delta \delta_f = -\Delta_\delta K_{fb} x$, the closed-loop system can be obtained as

$$A_{CL}(v_{\max}) = A(v_{\max}) - B\Delta_\delta K_{fb}. \tag{B2}$$

Given the tuning gain $\Delta_\delta > 0$ in the range $[\Delta_{\delta\min}, \Delta_{\delta\max}]$, we can define

$$\underline{A}_{CL} = A(v_{\max}) - B\Delta_{\delta\max} K_{fb} \tag{B3}$$

$$\bar{A}_{CL} = A(v_{\max}) - B\Delta_{\delta\min} K_{fb}. \tag{B4}$$

The closed-loop system (B-2) can be represented as a convex combination of $\underline{A}_{\mathrm{CL}}$ and $\bar{A}_{\mathrm{CL}}$, that is

$$A_{\mathrm{CL}}(v_{\max}) = \sigma \underline{A}_{\mathrm{CL}} + (1-\sigma)\bar{A}_{\mathrm{CL}} \tag{B5}$$

where σ is a parameter within the range [0, 1].

Defining the Lyapunov function candidate as $V = x^T P x$, its derivative with respect to time can be found as follows:

$$\begin{aligned}\dot{V} &= \dot{x}^T P x + x^T P \dot{x} \\ &= x^T (A_{CL}^T P + P A_{\mathrm{CL}}) x \\ &= \sigma x^T (\underline{A}_{\mathrm{CL}}^T P + P \underline{A}_{\mathrm{CL}}) x + (1-\sigma) x^T (\bar{A}_{\mathrm{CL}}^T P + P \bar{A}_{\mathrm{CL}}) x.\end{aligned}$$

Note that the designed feedback control K_{fb} is stable and the range of tuning gain Δ_δ is chosen to keep the closed-loop system stable, such that

$$\underline{A}_{\mathrm{CL}}^T P + P \underline{A}_{\mathrm{CL}} < 0 \tag{B6}$$

$$\bar{A}_{\mathrm{CL}}^T P + P \bar{A}_{\mathrm{CL}} < 0 \tag{B7}$$

for a positive matrix $P > 0$. Thus, the Lyapunov condition $\dot{V} < 0$ can be satisfied. Consequently, the stability of the FGS-compensated feedback control of the steering wheel controller can be assured under conditions (B6) and (B7).

Appendix C
Stability Consideration of SFGS Design

Let the longitudinal vehicle dynamics be a nonlinear system from the throttle or brake actuation to the vehicle velocity and acceleration [8], [10], [21]

$$\dot{x} = F(x,\ u) \tag{C1}$$

where $x = [v,\ \dot{v}]^T$ and u is the command degree to the throttle or brake actuator.

By expanding the system into a linearization state equation, (C1) can be written as

$$\dot{x} = A_0 v + B_0 u + g(x,\ u) \tag{C2}$$

where

$$A_0 = \left.\frac{\partial F}{\partial x}\right|_{(x_0,\ u_0)}, \quad B_0 = \left.\frac{\partial F}{\partial u}\right|_{(x_0,\ u_0)}$$

$(x_0,\ u_0)$ denotes the pair of the nominal operating point and nominal input, and $g(x, u)$ presents the higher order terms of (C1), in which uncertainties or disturbances are also included.

The fuzzy speed control system can be transformed into the so-called perturbed Lure system with uncertainties, as formed using (C2). By considering the fuzzy rule of SFLC in (34) and the fuzzy rule base in Table II, the controlling output u can be expressed as a nonlinear function, $u = \psi(D_s)$, which belongs to a sector [0, ρ], as depicted in Fig. 13. Note that $\psi(D_s)$ is, namely, the control surface of SFLC. The membership functions in SFLC determine the behavior of $\psi(\cdot)$, which is a time-invariant nonlinearity and must satisfy the sector condition in the defined universe, that is

$$\begin{aligned}&\psi(D_s)(\psi(D_s) - \rho D_s) \le 0 \\ &\text{with} \quad D_s = C_d(x_d - x),\ C_d = [k_p,\ k_d].\end{aligned} \tag{C3}$$

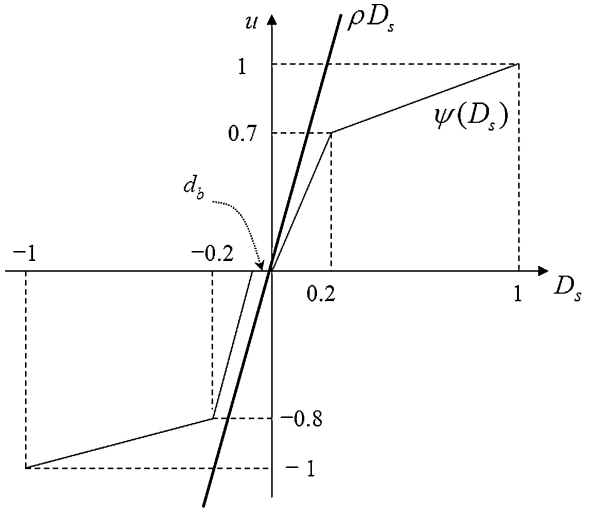

Fig. 13. Nonlinear feedback function of SFLC.

The nonlinearity $g(x, u)$ is bounded as follows:

$$||g(v,\ u)||_2 \le \frac{\varepsilon}{2||P||_2 + 2\eta\rho^2||C_d||_2^2}||v||_2 \tag{C4}$$

where P is a positive-definite symmetric matrix, and ε and η are positive constants.

In addition, $-(1/\eta)$ is not an eigenvalue of A_0 such that

$$\mathrm{Re}[1 + \rho(1+\eta s)G(s)] > 0 \tag{C5}$$

where

$$G(s) = C_d(sI - A_0)^{-1}B_0 \tag{C6}$$

and $(A_0,\ B_0,\ C_d)$ is the minimal realization of $G(s)$.

By applying Lyapunov's direct method, the stability of the system (C2) under the conditions from (C3) to (C6) can be guaranteed [36], [40]. Thus, the designed SFLC is absolutely stable.

References

[1] L. Li, X. Li, C. Cheng, C. Chen, G. Ke, D. D. Zeng, and W. T. Scherer, "Research collaboration and ITS topic evolution: 10 years at T-ITS," *IEEE Trans. Intell. Transportat. Syst.*, vol. 11, no. 3, pp. 517–523, Mar. 2010.

[2] D. Pomerleau, "RALPH: Rapidly adapting lateral position handler," in *Proc. IEEE Intell. Veh. Symp.*, Sep. 1995, pp. 506–511.

[3] D. Pomerleau, "Visibility estimation from a moving vehicle using the RALPH vision system," in *Proc. IEEE Intell. Transportat. Syst.*, Nov. 1997, pp. 906–911.

[4] M. Bertozzi and A. Broggi, "GOLD: A parallel real-time stereo vision system for generic obstacle and lane detection," *IEEE Trans. Image Process.*, vol. 7, no. 1, pp. 62–81, Jan. 1998.

[5] M. Bertozzi, A. Broggi, and A. Fascioli, "ARGO and the MilleMiglia in automatico tour," *IEEE Trans. Intell. Transportat. Syst.*, vol. 14, no. 1, pp. 55–64, Jan. 1999.

[6] T. Hessburg and M. Tomizuka, "Fuzzy logic control for lateral vehicle guidance," *IEEE Contr. Syst. Mag.*, vol. 14, no. 4, pp. 55–63, Aug. 1994.

[7] R. Horowitz, C. W. Tan, and X. Sun, "An efficient lane change maneuver for platoons of vehicles in an automated highway system," California Partners Adv. Transit Highways, Univ. California Berkeley, Berkeley, Working Rep. UCB-ITS-PRR-2004-16, May 2004.

[8] R. Rajamani, H. S. Tan, B. K. Law, and W. B. Zhang, "Demonstration of integrated longitudinal and lateral control for the operation of automated vehicles in platoon," *IEEE Trans. Contr. Syst. Technol.*, vol. 8, no. 4, pp. 695–708, Apr. 2000.

[9] H. Jula, E. B. Kosmatopoulos, and P. Ioannou, "Collision avoidance analysis for lane-change and merging," *IEEE Trans. Vehicul. Technol.*, vol. 49, no. 6, pp. 2295–2308, Nov. 2000.
[10] D. Swaroop, J. K. Hedrick, and S. B. Choi, "Direct adaptive longitudinal control of vehicle platoons," *IEEE Trans. Vehicul. Technol.*, vol. 50, no. 1, pp. 150–161, Jan. 2001.
[11] C. Hatipoglu, Ü. Özgüner, and K. A. Redmill, "Automated lane change controller design," *IEEE Trans. Intell. Transportat. Syst.*, vol. 4, no. 3, pp. 13–22, Mar. 2003.
[12] J. Farrell, H. S. Tan, and Y. Yang, "Carrier phase GPS-aided INS based vehicle lateral control," *Trans. ASME, J. Dyn. Syst. Meas. Contr.*, vol. 125, no. 3, pp. 339–353, 2003.
[13] J. Mar and H. T. Lin, "The car-following and lane-change collision prevention system based on the cascaded fuzzy inference system," *IEEE Trans. Vehicul. Technol.*, vol. 54, no. 3, pp. 910–924, May 2005.
[14] L. Cai, A. B. Rad, and W. L. Chan, "A genetic fuzzy controller for vehicle automatic steering control," *IEEE Trans. Vehicul. Technol.*, vol. 56, no. 2, pp. 529–543, Mar. 2007.
[15] J. E. Naranjo, C. Gonzalez, R. Garcia, and T. Pedro, "Lane-change fuzzy control in autonomous vehicles for the overtaking maneuver," *IEEE Trans. Intell. Transportat. Syst.*, vol. 9, no. 3, pp. 438–450, Sep. 2008.
[16] S. J. Wu, H. H. Chiang, J. W. Perng, C. J. Chen, B. F. Wu, and T. T. Lee, "The heterogeneous systems integration design and implementation for lane keeping on a vehicle," *IEEE Trans. Intell. Transportat. Syst.*, vol. 9, no. 2, pp. 246–263, Jun. 2008.
[17] M. S. Darms, P. E. Rybski, C. Baker, and C. Urmson, "Obstacle detection and tracking for the urban challenge," *IEEE Trans. Intell. Transportat. Syst.*, vol. 10, no. 3, pp. 475–485, Sep. 2009.
[18] R. Schubert, K. Schulze, and G. Wanielik, "Situation assessment for automatic lane-change maneuvers," *IEEE Trans. Intell. Transportat. Syst.*, vol. 11, no. 3, pp. 607–616, Sep. 2010.
[19] T. Shamir, "How should an autonomous vehicle overtake a slower moving vehicle: Design and analysis of an optimal trajectory," *IEEE Trans. Automat. Contr.*, vol. 49, no. 4, pp. 607–610, Apr. 2004.
[20] G. Usman and F. Kunwar, "Autonomous vehicle overtaking-an online solution," in *Proc. IEEE Int. Conf. Automat. Logist.*, Aug. 2009, pp. 596–610.
[21] S. Glaser, B. Vanholme, S. Mammar, D. Gruyer, and L. Nouveliere, "Maneuver-based trajectory planning for highly autonomous vehicles on real road with traffic and driver interaction," *IEEE Trans. Intell. Transportat. Syst.*, vol. 11, no. 3, pp. 589–606, Sep. 2010.
[22] I. Baturone, F. J. Moreno-Velo, V. Blanco, and J. Ferruz, "Design of embedded DSP-based fuzzy controllers for autonomous mobile robot," *IEEE Trans. Indust. Electron.*, vol. 55, no. 2, pp. 928–936, Feb. 2008.
[23] J. G. Juang, L. H. Chien, and F. Lin, "Automatic landing control system design using adaptive neural network and its hardware realization," *IEEE Syst. J.*, vol. 5, no. 2, pp. 266–277, Jun. 2011.
[24] C. M. Lin, M. H. Lin, and C. W. Chen, "SoPC-based adaptive PID control system design for magnetic levitation system," *IEEE Syst. J.*, vol. 5, no. 2, pp. 278–287, Jun. 2011.
[25] A. Stone, "An ontological approach to quantifying the functional flexibility of embedded systems," *IEEE Syst. J.*, vol. 5, no. 1, pp. 111–120, Mar. 2011.
[26] D. D. Salvucci, "Modeling driver behavior in a cognitive architecture," *Human Factors*, vol. 48, no. 2, pp. 362–380, 2006.
[27] H. H. Chiang, S. J. Wu, J. W. Perng, B. F. Wu, and T. T. Lee, "The human-in-the-loop design approach to the longitudinal automation system for an intelligent vehicle," *IEEE Trans. Syst., Man, Cybern. A, Syst., Humans*, vol. 40, no. 4, pp. 708–720, Jul. 2010.
[28] E. Azimirad, N. Pariz, and M. B. N. Sistani, "A novel fuzzy model and control of single intersection at urban traffic network," *IEEE Syst. J.*, vol. 4, no. 1, pp. 107–111, Mar. 2010.
[29] B. F. Wu, C. T. Lin, and Y. L. Chen, "Dynamic calibration and occlusion handling algorithms for lane tracking," *IEEE Trans. Industr. Electron.*, vol. 56, no. 5, pp. 1757–1773, May 2009.
[30] Y. L. Chen, B. F. Wu, H. Y. Huang, and C. J. Fan, "A real-time vision system for nighttime vehicle detection and traffic surveillance," *IEEE Trans. Industr. Electron.*, vol. 58, no. 5, pp. 2030–2044, May 2011.
[31] R. Rajamani, *Vehicle Dynamics and Control*. New York: Springer, 2006.
[32] J. H. Kim, S. Hayakawa, T. Suzuki, K. Hayashi, S. Okuma, N. Tsuchida, M. Shimizu, and S. Kido, "Modeling of driver's collision avoidance maneuver based on controller switching model," *IEEE Trans. Syst., Man, Cybern. B, Cybern.*, vol. 35, no. 6, pp. 1131–1143, Dec. 2005.
[33] P. Seiler, B. Song, and J. K. Hedrick, "Development of a collision avoidance system," in *Proc. SAE Conf.*, no. 98PC417. 1998, pp. 97–103.
[34] P. Cook, "Stable control of vehicle convoys for safety and comfort," *IEEE Trans. Automat. Contr.*, vol. 52, no. 3, pp. 526–531, Mar. 2007.
[35] Y. Yamaguchi and T. Murakami, "Adaptive control for virtual steering characteristics on electric vehicle using steer-by-wire system," *IEEE Trans. Industr. Electron.*, vol. 56, no. 5, pp. 1585–1594, May 2009.
[36] B. J. Choi, S. W. Kwak, and B. K. Kim, "Design stability analysis of single-input fuzzy logic controller," *IEEE Trans. Syst., Man, Cybern. B, Cybern.*, vol. 30, no. 2, pp. 303–309, Apr. 2000.
[37] *TMS320F2812 Event Manager (EV) Reference Guides*, Texas Instruments, Dallas, 2003.
[38] J. C. McCall and M. M. Trivedi, "Driver behavior and situation aware brake assistance for intelligent vehicles," *Proc. IEEE*, vol. 95, no. 2, pp. 374–387, Feb. 2007.
[39] D. Caveney, "Cooperative vehicular safety applications," *IEEE Contr. Syst. Mag.*, vol. 30, no. 4, pp. 38–53, Aug. 2010.
[40] H. Miyagi and K. Yamashita, "Robust stability of Lure systems with multiple nonlinearities," *IEEE Trans. Automat. Contr.*, vol. 37, no. 6, pp. 883–886, Jun. 1992.

Hsin-Han Chiang (S'02–M'04) received the B.S. and Ph.D. degrees in electrical and control engineering from the National Chiao Tung University, Hsinchu, Taiwan, in 2001 and 2007, respectively.

He was a Post-Doctoral Researcher in electrical engineering with the National Taipei University of Technology, Taipei, Taiwan, in 2008 and 2009. Since August 2009, he has been an Assistant Professor with the Department of Electrical Engineering, Fu Jen Catholic University, Hsinchuang, New Taipei City, Taiwan. His current research interests include fuzzy control systems, embedded systems, vehicle dynamics and control, wheeled mobile robots, and intelligent carrier systems.

Yen-Lin Chen (S'02–M'07–SM'12) was born in Kaohsiung, Taiwan, in 1978. He received the B.S. and Ph.D. degrees in electrical and control engineering from National Chiao Tung University, Hsinchu, Taiwan, in 2000 and 2006, respectively.

From February 2007 to July 2009, he was an Assistant Professor with the Department of Computer Science and Information Engineering, Asia University, Taichung, Taiwan. He is currently an Associate Professor with the Department of Computer Science and Information Engineering, National Taipei University of Technology, Taipei, Taiwan. His current research interests include image and video processing, pattern recognition, embedded systems, document image analysis, and intelligent transportation systems.

Dr. Chen was a recipient of the Dragon Golden Paper Award sponsored by the Acer Foundation and the Silver Award of the Technology Innovation Competition sponsored by AdvanTech in 2003. He is a member of IAPR and IEICE.

Bing-Fei Wu (S'89–M'92–SM'02–F'11) was born in Taipei, Taiwan, in 1959. He received the B.S. and M.S. degrees in control engineering from National Chiao Tung University, Hsinchu, Taiwan, in 1981 and 1983, respectively, and the Ph.D. degree in electrical engineering from the University of Southern California, Los Angeles, in 1992.

Since 1992, he has been with the Department of Electrical Engineering and Control Engineering, where he is currently a Professor. He has been involved in the research of intelligent transportation systems for many years and leads a research team to develop the first Taiwanese smart car, TAIWAN *i*TS-1, with autonomous driving and an active safety system. His current research interests include data compression, vision-based vehicle driving safety, intelligent vehicle control, multimedia signal analysis, and embedded systems and chip design.

Dr. Wu is a fellow of IET.

Tsu-Tian Lee (M'87–SM'89–F'97) received the B.S. degree in control engineering from the National Chiao Tung University (NCTU), Hsinchu, Taiwan, in 1970, and the M.S. and Ph.D. degrees in electrical engineering from the University of Oklahoma, Norman, in 1972 and 1975, respectively.

In 1975, he became an Associate Professor and in 1978, a Professor and the Chairman of the Department of Control Engineering, NCTU. In 1981, he became a Professor and the Director of the Institute of Control Engineering, NCTU. In 1986, he was a Visiting Professor and in 1987, a Full Professor of electrical engineering with the University of Kentucky, Lexington. In 1990, he was a Professor and the Chairman of the Department of Electrical Engineering, National Taiwan University of Science and Technology (NTUST), Taipei, Taiwan. In 1998, he was a Professor and the Dean of the Office of Research and Development, NTUST. Since 2000, he has been with the Department of Electrical and Control Engineering, NCTU, where he is currently the Chair Professor. From 2004 to 2010, he was the President of the National Taipei University of Technology (NTUT), Taipei. He is currently the Chair Professor of Chung Yuan Christian University, Taoyuan, Taiwan.

Prof. Lee was a recipient of the Distinguished Research Award from the National Science Council, Taiwan, in 1991–1998, the Academic Achievement Award in Engineering and Applied Science in 1997 and the National Endowed Chair in 2003, both from the Ministry of Education, Taiwan, and the TECO Science and Technology Award from TECO Technology Foundation in 2003. He was an IEE fellow in 2000 and a fellow of the New York Academy of Sciences in 2002. He was a Technical Program Committee Member and an Advisory Committee Member of many IEEE-sponsored international conferences. He is currently the Vice President of Membership, a member of the Board of Governors, and the Newsletter Editor of the IEEE Systems, Man, and Cybernetics Society.